Article

Strong Electronic Couplings between Ferrocenyl Centers Mediated by Bis-Ethynyl/Butadiynyl Diruthenium Bridges

Guo-Lin Xu, Robert J. Crutchley, Maria C. DeRosa, Qing-Jiang Pan, Hong-Xing Zhang, Xiaoping Wang, and Tong Ren

J. Am. Chem. Soc., **2005**, 127 (38), 13354-13363• DOI: 10.1021/ja0534452 • Publication Date (Web): 31 August 2005

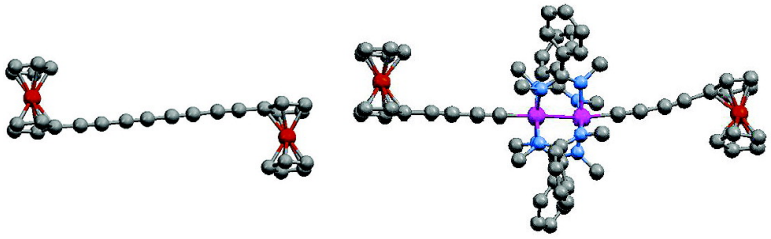

Fc-(C≡C)$_4$-Fc: Fc-Fc 11.7 Å apart and not coupled

Fc-(C≡C)$_2$-Ru$_2$-(C≡C)$_2$-Fc: Fc-Fc 16.7 Å apart, but strongly coupled

More About This Article

Additional resources and features associated with this article are available within the HTML version:

- Supporting Information
- Links to the 20 articles that cite this article, as of the time of this article download
- Access to high resolution figures
- Links to articles and content related to this article
- Copyright permission to reproduce figures and/or text from this article

View the Full Text HTML

J|A|C|S
ARTICLES
Published on Web 08/31/2005

Strong Electronic Couplings between Ferrocenyl Centers Mediated by Bis-Ethynyl/Butadiynyl Diruthenium Bridges

Guo-Lin Xu,[†] Robert J. Crutchley,*[,‡] Maria C. DeRosa,[‡] Qing-Jiang Pan,[§] Hong-Xing Zhang,[§] Xiaoping Wang,[||] and Tong Ren*[,†,⊥]

Contribution from the Departments of Chemistry, University of Miami, Coral Gables, Florida 33146, Carleton University, Ottawa, ON K1S 5B6, Canada, State Key Laboratory of Theoretical and Computational Chemistry, Institute of Theoretical Chemistry, Jilin University, Changchun 130023, P. R. China, and Texas A&M University, College Station, Texas 77842

Received May 26, 2005; E-mail: tren@purdue.edu

Abstract: A series of *trans*-(FcC_{2n})Ru_2(Y-DMBA)$_4$(C_{2m}Fc) with n, m = 1 and 2 and Y-DMBA as *N*,*N*′-dimethylbenzamidinate or *N*,*N*′-dimethyl-(3-methoxy)benzamidinate have been synthesized and characterized. The intramolecular Fc···Fc distances, established through single-crystal X-ray diffraction studies, range from 11.6 to 16.6 Å. Results from both voltammetric and spectroelectrochemical studies indicate that the (−C_{2n})Ru_2(Y-DMBA)$_4$(C_{2m}−) fragments are among the most efficient mediators of intramolecular *hole* transfer. Density-functional calculations offer both the insight on the ground-state electronic properties and unambiguous assignment for the observed electronic absorptions.

Introduction

Charge transfer (CT) processes are paramount to both chemistry and biology and have been extensively researched for the past fifty years.[1−4] In addition to the research of intramolecular CT processes in bulk media, recent years have witnessed a new thrust to understand CT processes on the nanoscale,[5] especially with respect to active molecules in molecular electronic devices.[6] Linear conjugated molecules, both organic and inorganic, are among the most thoroughly investigated. Transition metal complexes containing σ-polyynyl ligand have been studied in many laboratories as potential molecular wires.[7−14] Notable metal complex units that lead to significant electronic couplings across polyyn-diyl bridges judged from voltammetric data include CpRe(P)(NO) (P denotes monodentate phosphines),[15−17] $CpFe(P)_2$ and CpFe(P—P) (P—P denotes bidentate phosphines),[18,19] $CpRu(P)_2$,[20,21] CpRu(P—P),[22] and $MnI(P—P)_2$ and CpMn(P—P).[23,24] Emissive dimetallic compounds bridged by polyyn-diyl, so-called "molecular photonic wires", are also known with metal centers such as Re(I), Pt(II), and Au(I).[25−27] Further illustrating the promise of metal-alkynyl species as molecular wires, several *trans*-$PtP_2(C{\equiv}CPh)_2$ type compounds were found to be more conductive than the oligo(phenyleneethynes) of comparable length.[28] Our interests in this area focus on diruthenium-alkynyl compounds,[29,30] and recent

[†] University of Miami.
[‡] Carleton University.
[§] Jilin University.
[||] Texas A&M University.
[⊥] Current address: Department of Chemistry, Purdue University, West Lafayette, IN 47907.

(1) Marcus, R. A.; Sutin, N. *Biochim. Biophys. Acta* **1985**, *811*, 265.
(2) Barbara, P. F.; Meyer, T. J.; Ratner, M. A. *J. Phys. Chem.* **1996**, *100*, 13148.
(3) Endicott, J. F. *Comprehensive Coordination Chemistry II: From Biology to Nanotechnology*; Elsevier/Pergamon: Oxford, 2004; Vol. 7.
(4) Creutz, C.; Brunschwig, B. S.; Sutin, N. *Comprehensive Coordination Chemistry II: From Biology to Nanotechnology*; Elsevier/Pergamon: Oxford; New York, 2004; Vol. 7.
(5) Adams, D. M. et al. *J. Phys. Chem. B* **2003**, *107*, 6668.
(6) *Molecular Nanoelectronics*; Reed, M. A., Lee, T., Eds.; American Scientific Publishers: Stevenson Ranch, CA, 2003.
(7) Bruce, M. I.; Low, P. J. *Adv. Organomet. Chem.* **2004**, *50*, 179.
(8) Low, P. J.; Bruce, M. I. *Adv. Organomet. Chem.* **2001**, *48*, 71.
(9) Paul, F.; Lapinte, C. *Coord. Chem. Rev.* **1998**, *178−180*, 431.
(10) Paul, F.; Lapinte, C. In *Unusual Structures and Physical Properties in Organometallic Chemistry*; Gielen, M., Willem, R., Wrackmeyer, B., Eds.; Wiley: West Sussex, 2002.
(11) Chisholm, M. H. *Angew. Chem., Int. Ed. Engl.* **1991**, *30*, 673.
(12) Bunz, U. H. F. *Angew. Chem., Int. Ed. Engl.* **1996**, *35*, 969.
(13) Manna, J.; John, K. D.; Hopkins, M. D. *Adv. Organomet. Chem.* **1995**, *38*, 79.
(14) Long, N. J.; Williams, C. K. *Angew. Chem., Int. Ed.* **2003**, *42*, 2586.
(15) Batrik, T.; Bartik, B.; Brady, M.; Dembinski, R.; Gladysz, J. A. *Angew. Chem., Int. Ed. Engl.* **1996**, *35*, 414.
(16) Brady, M.; Weng, W.; Zou, Y.; Seyler, J. W.; Amoroso, A. J.; Arif, A. M.; Bohme, M.; Frenking, G.; Gladysz, J. A. *J. Am. Chem. Soc.* **1997**, *119*, 775.
(17) Dembinski, R.; Bartik, T.; Bartik, B.; Jaeger, M.; Gladysz, J. A. *J. Am. Chem. Soc.* **2000**, *122*, 810.
(18) Coat, F.; Lapinte, C. *Organometallics* **1996**, *15*, 477.
(19) Coat, F.; Paul, F.; Lapinte, C.; Toupet, L.; Costuas, K.; Halet, J.-F. *J. Organomet. Chem.* **2003**, *683*, 368.
(20) Bruce, M. I.; Low, P. J.; Costuas, K.; Halet, J.-F.; Best, S. P.; Heath, G. A. *J. Am. Chem. Soc.* **2000**, *122*, 1949.
(21) Bruce, M. I.; Costuas, K.; Halet, J.-F.; Hall, B. C.; Low, P. J.; Nicholson, B. K.; Skelton, B. W.; White, A. H. *J. Chem. Soc., Dalton Trans.* **2002**, 383.
(22) Gao, L.-B.; Zhang, L.-Y.; Shi, L.-X.; Chen, Z.-N. *Organometallics* **2005**, *24*, 1678.
(23) Kheradmandan, S.; Heinze, K.; Schmalle, H. W.; Berke, H. *Angew. Chem., Int. Ed.* **1999**, *38*, 2270.
(24) Fernández, F. J.; Venkatesan, K.; Blacque, O.; Alfonso, M.; Schmalle, H. W.; Berke, H. *Chem.—Eur. J.* **2003**, *9*, 6192.
(25) Yam, V. W. W.; Lau, V. C. Y.; Cheung, K. K. *Organometallics* **1996**, *15*, 1740.
(26) Yam, V. W.-W.; Wong, K. M.-C.; Zhu, N. *Angew. Chem., Int. Ed.* **2003**, *42*, 1400.
(27) Che, C. M.; Chao, H. Y.; Miskowski, V. M.; Li, Y. Q.; Cheung, K. K. *J. Am. Chem. Soc.* **2001**, *123*, 4985.
(28) Schull, T. L.; Kushmerick, J. G.; Patterson, C. H.; George, C.; Moore, M. H.; Pollack, S. K.; Shashidhar, R. *J. Am. Chem. Soc.* **2003**, *125*, 3202.

10.1021/ja0534452 CCC: $30.25

Scheme 1. Ru_2-alkynyl oligomers.

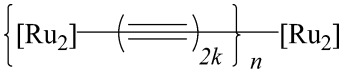

significant results include the demonstration of *electron* mobility across both the polyyn-diyl and *E*-hex-3-ene-1,5-diyn-diyl linkers between two Ru_2 units.[31−33] Ultimately, we hope to succeed in the synthesis of monodisperse oligomers of Ru_2-alkynyl monomers (Scheme 1) and to realize molecular wires of precisely controlled lengths.

We have shown in previous studies[31,32,34] that the oligomer outlined in Scheme 1 can mediate facile charge transfer across the Ru_2 unit and the carbon-rich bridges and therefore possess the desired properties of a molecular wire. Probing the efficiency of charge transfer across a metal unit ({M}) is a key element of purposeful design. One of the commonly invoked techniques is to attach a pair of identical electroactive reporter groups (X) at the opposite ends of {M} and use both the free energy of comproportionation ($\Delta G_c = F\Delta E_c$, and ΔE_c is defined by eqs 1 and 2) and spectroscopic characteristics of the mixed-valence ion $[X-\{M\}-X]^{\pm 1}$ to gauge the *hole* (oxidation) or *electron* (reduction) mobility across {M}:[35]

$$X-\{M\}-X \underset{E_{1/2(I)}}{\overset{-e^-}{\rightleftharpoons}} [X-\{M\}-X]^+ \underset{E_{1/2(II)}}{\overset{-e^-}{\rightleftharpoons}} [X-\{M\}-X]^{2+} \quad (1a)$$

$$X-\{M\}-X \underset{E_{1/2(I)}}{\overset{+e^-}{\rightleftharpoons}} [X-\{M\}-X]^- \underset{E_{1/2(II)}}{\overset{+e^-}{\rightleftharpoons}} [X-\{M\}-X]^{2-} \quad (1b)$$

$$\Delta E_c = |[E_{1/2}(II) - E_{1/2}(I)]| \quad (2)$$

Ferrocenes and other metallocenes are among the most popular choices of reporter groups, and their applications have been reviewed.[35,36] The ferrocenylethynyl group (FcC≡C) is particularly attractive in assessing charge mobility between metal centers because of the σ- and π-bonding capacity of ethynyl to a bridging transition metal. The first example of ferrocenylethynyl as the probe appears to be the study of *trans*-$Pt(PR_3)_2(C{\equiv}CFc)_2$ by Osella,[37,38] where a ΔE_c of 80 mV was estimated from cyclic voltammetry (CV). Reported concurrently by groups of Long[39] and Wolf,[40,41] *trans*-$Ru(dppm)_2(C{\equiv}CFc)_2$ was shown to have a ΔE_c of 220 mV and its mixed valent cation, $[trans\text{-}Ru(dppm)_2(C{\equiv}CFc)_2]^+$, was assigned as a Robin−Day class II species based on its spectral signatures. Yip et al. reported ΔE_c values of 110 and 270 mV for $[Cu_3(dppm)_3(\mu_3\text{-}\eta^1\text{-}C{\equiv}CFc)_2]^+$ and *trans*-$Pt_2(dppm)_2(C{\equiv}CFc)_2$,

Scheme 2. Compounds **1** (Y = H) and **2** (Y = OCH_3)

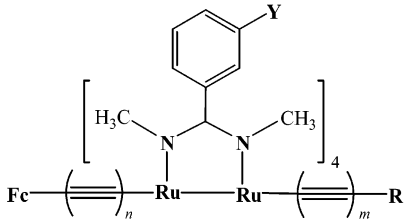

	1a/2a	**1b/2b**	**1c/2c**	**2d**
n =	1	1	2	1
m =	1	2	2	1
R =	Fc	Fc	Fc	Si^iPr_3

respectively, and the class II assignment for the mixed valent species in both cases.[42,43] Adams et al. also documented modest electronic couplings between two Fc units in various Os-carbonyl clusters bearing π-bonded $Fc(C{\equiv}C)_nFc$ ligand.[44−46] Similar electronic coupling in Ru-carbonyl clusters was observed by Bruce et al.[47] Very recently, Cotton et al. reported a novel linear trimetallic species, *trans*-$Co_3(dpa)_4(C{\equiv}CFc)_2$, for which a ΔE_c of 70 mV was indirectly estimated from CV data.[48] It is also worth noting that many compounds containing two σ-FcC≡C ligands have been reported for which either electrochemistry was not interrogated or no discernible ΔE_c was observed.[49−60]

In the preceding communication, we established through both voltammetric and spectroelectrochemical measurements that two Fc moieties are strongly coupled in the *trans*-$Ru_2(Y\text{-}DMBA)_4(C_2Fc)_2$ type compounds (Y-DMBA are *m*-substituted dimethylbenzamidinates, **1a**/**2a** in Scheme 2).[34] Described in this contribution are, in addition to the details about compounds **1a**/**2a**, the syntheses and structural characterizations of both the symmetric bis-ferrocenylbutadiynyl (FcC_4, **1c**/**2c** in Scheme 2) and unsymmetric FcC_2/FcC_4 adducts (**1b**/**2b**) of the $Ru_2(Y\text{-}DMBA)_4$ core, the detailed voltammetric and spectroelectrochemical investigation of charge transport properties within these compounds, and a time-dependent density functional (TD-DFT) calculation of the model compound *trans*-$Ru_2(NHCHNH)_4(C{\equiv}CFc)_2$ (**3**) that provides insights on spectral assignment for compounds **1** and **2**.

(29) Ren, T.; Xu, G.-L. *Comm. Inorg. Chem.* **2002**, *23*, 355.
(30) Hurst, S. K.; Ren, T. *J. Organomet. Chem.* **2003**, *670*, 188.
(31) Ren, T.; Zou, G.; Alvarez, J. *Chem. Commun.* **2000**, 1197.
(32) Xu, G.-L.; Zou, G.; Ni, Y.-H.; DeRosa, M. C.; Crutchley, R. J.; Ren, T. *J. Am. Chem. Soc.* **2003**, *125*, 10057.
(33) Shi, Y.; Yee, G. T.; Wang, G.; Ren, T. *J. Am. Chem. Soc.* **2004**, *126*, 10552.
(34) Xu, G.-L.; DeRosa, M. C.; Crutchley, R. J.; Ren, T. *J. Am. Chem. Soc.* **2004**, *126*, 3728.
(35) Barlow, S.; O'Hare, D. *Chem. Rev.* **1997**, *97*, 637.
(36) Zanello, P. In *Ferrocenes: Homogeneous Catalysis, Organic Synthesis, Materials Science*; Togni, A., Hayashi, T., Eds.; VCH: New York, 1995.
(37) Osella, D.; Gambino, O.; Nervi, C.; Ravera, M.; Russo, M. V.; Infante, G. *Inorg. Chim. Acta* **1994**, *225*, 35.
(38) Osella, D.; Gobetto, R.; Nervi, C.; Ravera, M.; D'Amato, R.; Russo, M. V. *Inorg. Chem. Commun.* **1998**, *1*, 239.
(39) Colbert, M. C. B.; Lewis, J.; Long, N. J.; Raithby, P. R.; White, A. J. P.; Williams, D. J. *J. Chem. Soc., Dalton Trans.* **1997**, 99.
(40) Jones, N. D.; Wolf, M. O.; Giaquinta, D. M. *Organometallics* **1997**, *16*, 1352.
(41) Zhu, Y.; Clot, O.; Wolf, M. O.; Yap, G. P. A. *J. Am. Chem. Soc.* **1998**, *120*, 1812.
(42) Yip, J. H. K.; Wu, J.; Wong, K.-Y.; Yeung, K.-W.; Vittal, J. J. *Organometallics* **2002**, *21*, 1612.
(43) Yip, J. H. K.; Wu, J.; Wong, K.-Y.; Ho, K. P.; Pun, C. S.-N.; Vittal, J. J. *Organometallics* **2002**, *21*, 5292.
(44) Adams, R. D.; Qu, B. *Organometallics* **2000**, *19*, 2411.
(45) Adams, R. D.; Qu, B.; Smith, M. D. *J. Organomet. Chem.* **2001**, *637*−*639*, 514.
(46) Adams, R. D.; Qu, B.; Smith, M. D.; Albright, T. A. *Organometallics* **2002**, *21*, 2970.
(47) Bruce, M. I.; Skelton, B. W.; White, A. H.; Zaitseva, N. N. *J. Organomet. Chem.* **2002**, *650*, 188.
(48) Berry, J. F.; Cotton, F. A.; Murillo, C. A. *Organometallics* **2004**, *23*, 2503.
(49) Onitsuka, K.; Tao, X. Q.; Sonogashira, K. *Bull. Chem. Soc. Jpn.* **1994**, *67*, 2611.
(50) Back, S.; Rheinwald, G.; Zsolnai, L.; Huttner, G.; Lang, H. *J. Organomet. Chem.* **1998**, *563*, 73.
(51) Back, S.; Pritzkow, H.; Lang, H. *Organometallics* **1998**, *17*, 41.
(52) Back, S.; Rheinwald, G.; Lang, H. *Organometallics* **1999**, *18*, 4119.
(53) Belen'kaya, A. G.; Dolgushin, F. M.; Peterleitner, M. G.; Petrovskii, P. V.; Krivykh, V. V. *Russ. Chem. Bull.* **2002**, *51*, 170.
(54) Back, S.; Rheinwald, G.; Lang, H. *J. Organomet. Chem.* **2000**, *601*, 93.
(55) Lang, H.; Mansilla, N.; Rheinwald, G. *Organometallics* **2001**, *20*, 1592.
(56) Herberhold, M.; Schmalz, T.; Milius, W.; Wrackmeyer, B. *J. Organomet. Chem.* **2002**, *641*, 173.
(57) Bruce, M. I.; Zaitseva, N. N.; Skelton, B. W.; Somers, N.; White, A. H. *Aust. J. Chem.* **2003**, *56*, 509.
(58) Wei, Q.-H.; Zhang, L.-Y.; Shi, L.-X.; Chen, Z.-N. *Inorg. Chem. Commun.* **2004**, *7*, 286.
(59) Yip, J. H. K.; Wu, J.; Wong, K.-Y.; Ho, K. P.; Koh, L. L.; Vittal, J. J. *Eur. J. Inorg. Chem.* **2004**, 1056.
(60) Zhu, Y. B.; Wolf, M. O. *J. Am. Chem. Soc.* **2000**, *122*, 10121.

Scheme 3. Synthetic route to the Fc-capped unsymmetric compounds

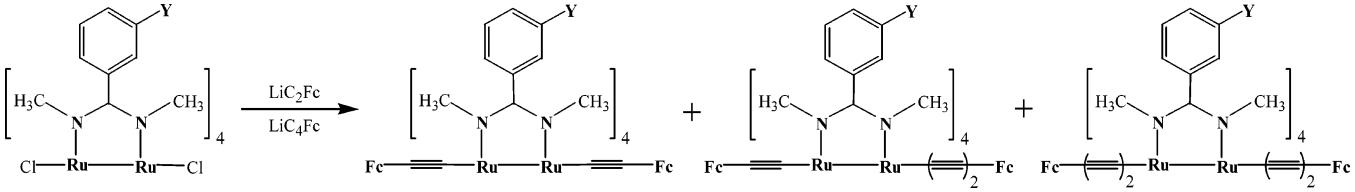

Results and Discussion

Synthesis. Similar to the synthesis of $Ru_2(DMBA)_4(C_2R)_2$ type compounds previously described,[61,62] reactions between $Ru_2(Y\text{-}DMBA)_4Cl_2$ and 5 equiv of LiC_2Fc or LiC_4Fc afforded symmetric compounds $Ru_2(Y\text{-}DMBA)_4(C_2Fc)_2$ (**1a**/**2a**) or $Ru_2(Y\text{-}DMBA)_4(C_4Fc)_2$ (**1c**/**2c**), respectively, in excellent yields. As shown in Scheme 3, the synthesis of the unsymmetric compounds **1b**/**2b** was effected with a reaction between $Ru_2(Y\text{-}DMBA)_4Cl_2$ and a mixture of LiC_2Fc and LiC_4Fc and subsequent chromatographic purification to separate the symmetric compounds **1a/2a** (trace) and **1c/2c** (minor) from the desired products (**1b**/**2b**). Similarly, the reaction between $Ru_2(m\text{-}MeODMBA)_4Cl_2$ and a mixture of LiC_2Fc and $LiC_2Si^iPr_3$ and the ensuing chromatographic purification resulted in the mono-Fc compound $Ru_2(m\text{-}MeODMBA)_4(C_2Si^iPr_3)(C_2Fc)$ (**2d**). Compounds **1** and **2** are all red crystalline, diamagnetic materials that display well resolved ^1H NMR spectra. The formation of unsymmetric compounds **1b**/**2b** was verified by the existence of two sets of Fc protons in their ^1H NMR spectra.

Molecular Structures. Although the presence of the *m*-MeO phenyl substituent greatly enhances the solubility of compounds **2a**−**2d** in organic solvents, it makes the growth of single crystals of X-ray quality very difficult. On the other hand, the less soluble compounds **1a**−**1c** crystallized readily and their crystal structures were determined via single-crystal X-ray diffraction. The structural plots of compounds **1a**−**1c** are shown in Figures 1−3, respectively, while the selected bond lengths and angles

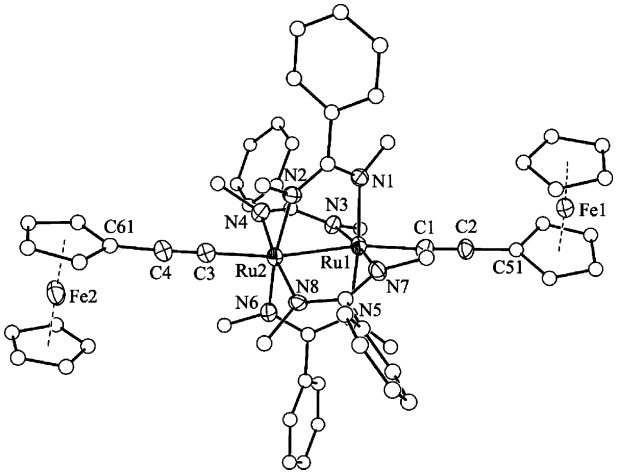

Figure 1. ORTEP plot of **1a** at 30% probability level. Hydrogen atoms were omitted for clarity.

are listed in Table 1. The structure of **1a** displays basic features expected for $Ru_2(DMBA)_4$-based bis-alkynyl compounds: two FcC≡C ligands occupy the opposite axial positions with the formation of strong σ(Ru—C) bonds (ca.1.98 Å). The formation of strong Ru—C bonds implies the polarization of the d_σ orbital on Ru centers toward the carbon center, which results in the loss of σ(Ru—Ru) and the elongation of the Ru—Ru bond (2.4386(9)−2.4544(9) Å in **1a**−**1c**) compared with that of the parent compound $Ru_2(DMBA)_4Cl_2$ (2.3224 Å).[61] The comparison of structural plots and tabulated data for compounds **1b**

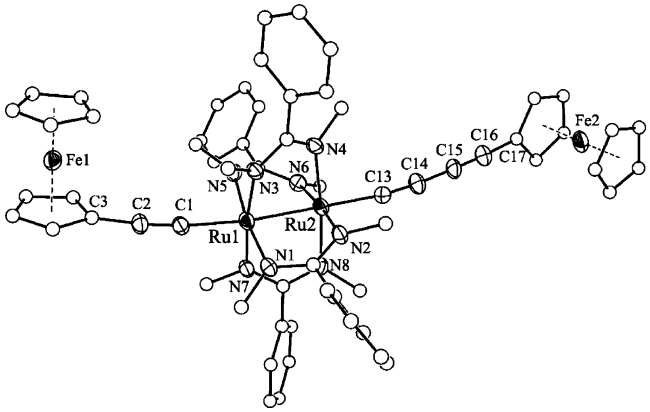

Figure 2. ORTEP plot of **1b** at 30% probability level. Hydrogen atoms were omitted for clarity.

and **1c** with those of **1a** revealed that the successive extensions of the conjugated backbone by one acetylene unit at a time has a minimal effect on both the Ru—Ru bond lengths and the coordination environment around the Ru_2 core.

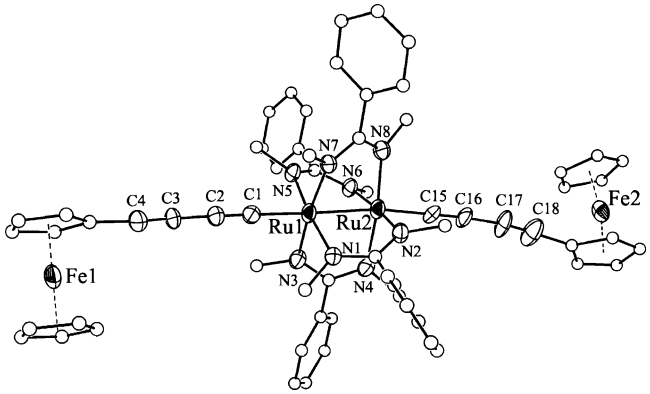

Figure 3. ORTEP plot of **1c** at 30% probability level. Both hydrogen atoms and the less populated orientation of the disordered Fc unit were omitted for clarity.

Inspection of structural data for **1a** and **1b** revealed both a large variation in Ru−N bond lengths and a significant deviation from linearity in Ru′−Ru−C angles. These distortions from an idealized D_{4h} geometry have been attributed to a second-order Jahn−Teller effect and documented in many bis-alkynyl compounds of a Ru_2(III,III) core.[61−64] Interestingly, compound **1c**

(61) Xu, G.-L.; Campana, C.; Ren, T. *Inorg. Chem.* **2002**, *41*, 3521.
(62) Hurst, S. K.; Xu, G.-L.; Ren, T. *Organometallics* **2003**, *22*, 4118.
(63) Lin, C.; Ren, T.; Valente, E. J.; Zubkowski, J. D. *J. Chem. Soc., Dalton Trans.* **1998**, 571.
(64) Xu, G.-L.; Jablonski, C. G.; Ren, T. *J. Organomet. Chem.* **2003**, *683*, 388.

Table 1. Selected Bond Lengths (Å) and Angles (deg) for Molecules **1a**−**1c**

1a		1b		1c	
Ru1−Ru2	2.4386(9)	Ru1−Ru2	2.4538(7)	Ru1−Ru2	2.4472(5)
Ru1−N1	2.034(7)	Ru1−N1	1.988(5)	Ru1−N1	2.034(4)
Ru1−N3	2.107(7)	Ru1−N3	2.002(5)	Ru1−N3	2.055(4)
Ru1−N5	2.035(6)	Ru1−N5	2.119(5)	Ru1−N5	2.054(4)
Ru1−N7	1.986(6)	Ru1−N7	2.070(7)	Ru1−N7	2.058(4)
Ru2−N2	2.007(6)	Ru2−N2	2.102(5)	Ru2−N2	2.038(4)
Ru2−N4	2.001(7)	Ru2−N4	2.067(5)	Ru2−N4	2.066(5)
Ru2−N6	2.050(7)	Ru2−N6	1.980(5)	Ru2−N6	2.036(4)
Ru2−N8	2.118(6)	Ru2−N8	2.008(5)	Ru2−N8	2.039(5)
Ru1−C1	1.981(8)	Ru1−C1	1.977(6)	Ru1−C1	1.977(3)
Ru2−C3	1.977(9)	Ru2−C13	1.977(6)	Ru2−C15A/B	1.945(5)/1.995(4)
C1−C2	1.193(11)	C1−C2	1.206(8)	C1−C2	1.201(1)
C3−C4	1.197(12)	C13−C14	1.194(8)	C15A−C16A	1.203(2)
Fe1···Fe2	14.21	Fe1···Fe2	16.58	Fe1···Fe2A/B[b]	19.44/19.61
$C_\omega\cdots C_\omega'$[a]	11.58	$C_\omega\cdots C_\omega'$[a]	13.84	$C_\omega\cdots C_\omega'$(A/B)[a,b]	16.58/16.67
C1−Ru1−Ru2	169.9(3)	C1−Ru1−Ru2	163.4(2)	C1−Ru1−Ru2	178.1(2)
Ru1−Ru2−C3	168.4(3)	Ru1−Ru2−C13	169.3(2)	Ru1−Ru2−C15A	172.2(5)
N1−Ru1−Ru2	86.17(18)	N1−Ru1−Ru2	92.80(13)	N1−Ru1−Ru2	86.94(11)
N3−Ru1−Ru2	81.23(18)	N3−Ru1−Ru2	89.67(13)	N3−Ru1−Ru2	87.25(12)
N5−Ru1−Ru2	86.74(18)	N5−Ru1−Ru2	79.27(13)	N5−Ru1−Ru2	85.81(11)
N7−Ru1−Ru2	92.73(18)	N7−Ru1−Ru2	83.46(13)	N7−Ru1−Ru2	85.32(11)
N2−Ru2−Ru1	87.50(18)	N2−Ru2−Ru1	80.26(13)	N2−Ru2−Ru1	85.94(11)
N4−Ru2−Ru1	92.16(19)	N4−Ru2−Ru1	83.99(13)	N4−Ru2−Ru1	85.16(12)
N6−Ru2−Ru1	86.10(19)	N6−Ru2−Ru1	93.40(14)	N6−Ru2−Ru1	87.18(11)
N8−Ru2−Ru1	80.01(17)	N8−Ru2−Ru1	89.34(13)	N8−Ru2−Ru1	87.42(11)
N1−Ru1−Ru2−N2	19.2(3)	N1−Ru1−Ru2−N2	20.6(2)	N1−Ru1−Ru2−N2	20.0(2)
N3−Ru1−Ru2−N4	19.7(3)	N3−Ru1−Ru2−N4	19.1(2)	N3−Ru1−Ru2−N4	21.1(2)
N5−Ru1−Ru2−N6	19.8(3)	N5−Ru1−Ru2−N6	21.1(2)	N7−Ru1−Ru2−N8	19.2(2)
N7−Ru1−Ru2−N8	21.1(3)	N7−Ru1−Ru2−N8	20.5(2)	N5−Ru1−Ru2−N6	20.7(2)
Fe1−C51···C61−Fe2	161.9	Fe1−C3···C17−Fe2	103.6	Fe1−C5···C19A/B−Fe2A/B	166.3/107.3

[a] C_ω and C_ω denote the Cp carbon atoms covalently bonded to the C≡C unit. [b] A/B denotes two different orientations

has a much narrower range in Ru−N bond lengths and almost linear Ru′−Ru−C angles despite the disorder of one Fc unit (see the description of the disorder in Experimental Section). All three compounds exhibit large N′−Ru′−Ru−N twisting angles (ca. 20°), which are due to the crowding within each DMBA bridge. The relative orientation between two Fc moieties (defined by the Fe−$C_\omega\cdots C_\omega'$−Fe′ twisted angle with C_ω and C_ω' as the Fc carbon centers bonded to the acetylene unit) is also interesting: they are almost trans to each other in **1a** (162°), close to orthogonal in **1b** (104°); and both nearly trans (166°) and orthogonal (107°) conformers are present due to the disorder of one of the Fc units (Fe2) in **1c**. The large variation in the relative orientation indicates that the observed Fe−$C_\omega\cdots C_\omega'$−Fe′ angles are determined by subtle crystal packing forces, and the free rotation of the FcC_{2n} moiety around the Ru−Ru axis in solution renders this parameter less relevant to Fc···Fc charge transfer. Both the edge−edge distance between two Fc centers ($C_\omega\cdots C_\omega'$) and Fe···Fe′ distances calculated from structural data are 11.6 and 14.2, 13.8 and 16.6, and 16.6 and 19.5 Å for compounds **1a**, **1b**, and **1c**, respectively.

Voltammetric Properties of Compounds 1 and 2. Both the differential pulse voltammograms (DPV) and cyclic voltammograms (CV) of compounds **2a**−**2d** recorded in THF are shown in Figure 4, while those of compounds **1a**−**1c** are provided in the Supporting Information. Compounds **1a**/**2a** exhibit four one-electron redox couples in the potential window of −1.5 V to +1.5 V (versus Ag/AgCl): (i) a reduction (**A**) at ∼ −1.2 V attributed to the $Ru_2(6+/5+)$ couple based on the comparison with the previous study of bis(alkynyl) adducts;[61,62,64] and (ii) three oxidations (**B**−**D**) between 0.4 and 1.0 V. As elucidated in the preliminary communication[34] and discussed in detail below, the least positive couple (**B**) is assigned as the $Ru_2(7+/6+)$ couple and the next two (**C** and

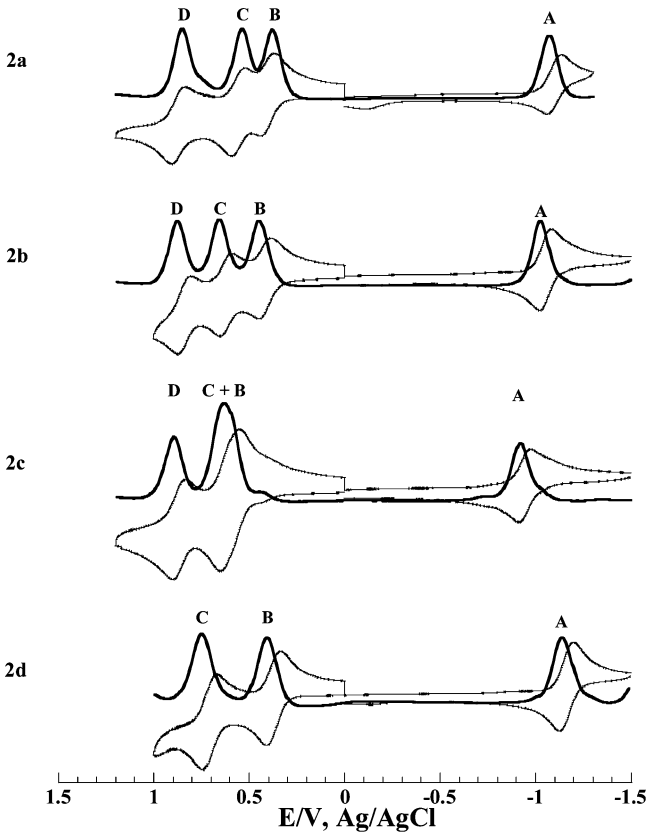

Figure 4. Differential pulse voltammograms (DPV, thick lines) and cyclic voltammograms (CV, thin gray lines) of compounds **2a**−**2d** recorded in 0.20 M THF solution of Bu_4NPF_6.

D) are designated as the Fc(+1/0) couples. These assignments are also illustrated in eq 3 below. The unsymmetric FcC_4/FcC_2 compound (**2b**) exhibits a pattern in voltammograms very

Table 2. Electrode Potentials (V) of **1a**−**c** and **2a**−**d** from DPV Measurements

	$Ru_2^{6+/5+}$ (**A**)	$Ru_2^{7+/6+}$ (**B**)	$[Fc-Fc]^{+1/0}$ (**C**)	$[Fc-Fc]^{+2/+1}$ (**D**)	E(**D**) − E(**C**)
1a	−1.136	0.324	0.476	0.772	0.296
1b	−1.032	0.400	0.609	0.816	0.207
1c	−0.932	0.596 (2 e^-)		0.864	0.268*
2a	−1.072	0.384	0.540	0.852	0.312
2b	−1.024	0.452	0.660	0.876	0.216
2c	−0.924	0.628(2 e^-)		0.900	0.272[a]
2d	−1.144	0.408	0.748 (1-e^-)		NA

[a] Calculated from the difference between E(**D**) and E(**B** and **C**).

similar to that of **2a** but with all couples positively shifted, reflecting the addition of an acetylenic unit that is strongly electron-withdrawing. For the symmetric bis-FcC_4 compound (**2c**), both the **A** and **D** couples exhibit a small but notable positive shift from that of **2b** as expected. On the other hand, the positive shift of the $Ru_2(7+/6+)$ couple in **2c** is so drastic that it significantly overlaps with the first Fc(+1/0) couple (**C**) to yield an apparent 2-e^- wave. The "accidental degeneracy" of **B** and **C** couples was also observed for compound **1c**. For the mono-Fc compound **2d**, the potentials of couples **A** and **B** are very close to those of corresponding couples in **2a**, while the potential of couple **C** is approximately the average of those of **C** and **D** couples in **2a**. Gathered in Table 2 are both the potential data of all compounds (**1a**−**c** and **2a**−**d**) from DPV measurements and the calculated potential difference between **C** and **D** couples (ΔE_{D-C}) as defined in eq 2.

$$[Fc-Ru_2^{III,II}-Fc]^{1-} \underset{A}{\overset{-e^-}{\rightleftharpoons}} Fc-Ru_2^{III,III}-Fc \underset{B}{\overset{-e^-}{\rightleftharpoons}} [Fc-Ru_2^{III,IV}-Fc]^{+} \underset{C}{\overset{-e^-}{\rightleftharpoons}} [Fc-Ru_2^{III,IV}-Fc^+]^{2+} \underset{D}{\overset{-e^-}{\rightleftharpoons}} [Fc^+-Ru_2^{III,IV}-Fc^+]^{3+} \quad (3)$$

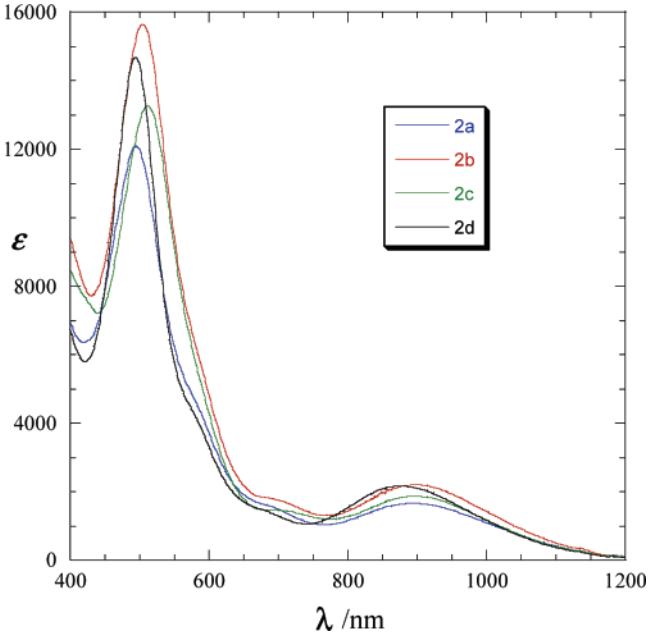

Figure 5. Vis−NIR absorption spectra of compounds **2a**−**2d** recorded in THF.

Electronic Spectroscopy and Structures. As shown in Figure 5 for compounds **2a**−**2d**, electronic absorption spectra of compounds **1** and **2** consist of two intense peaks at ca. 510 nm (ν_{max}, 19 600 cm^{-1}) and 910 nm (ν_{max}, 11 000 cm^{-1}), which are similar to those observed earlier for other $Ru_2(DMBA)_4(C_2Y)_2$ (Y = Ar or SiR_3) and $Ru_2(DMBA)_4(C_4Y)_2$ type compounds.[61,62,64] Ferrocenylethyne moieties are known to absorb weakly in the visible region (ϵ(448 nm) = 300),[65,66] but these transitions are masked by the intense peak around 510 nm in compounds **2**. The phenomenological assignments of optical transitions in diruthenium species are often impossible to make due to the pseudo-degeneracy of $\pi^*(Ru_2)$ and $\delta^*(Ru_2)$ orbitals.[67] The presence of two ferrocenyl groups further compounded the issue.

Scheme 4. Model Compound **3**[a]

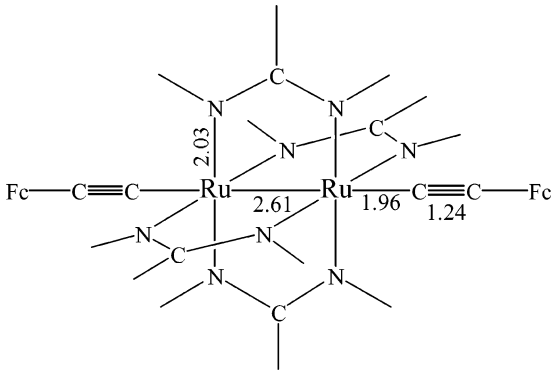

[a] Hydrogen atoms (open ends) omitted for the sake of clarity; Some optimized bond lengths are marked in Å.

To facilitate a reliable spectral assignment, density-functional calculations at the B3LYP/LanL2DZ level were performed on the model compound **3** shown in Scheme 4. The computation was simplified by the replacement of Y-DMBA ligands with $HNC(H)NH^{-1}$, which is a reasonable approximation since the phenyl ring is always orthogonal to the amidinate plane (N−C−N), and previous studies revealed the absence of significant electronic effect due to the phenyl ring.[62] The key optimized bond lengths are marked in Scheme 4, and the details about the optimized structure are provided in the Supporting Information. Most of the optimized bond lengths around Ru_2 agree well with those determined from X-ray studies with the exception of the Ru−Ru bond length that is about 0.15 Å longer than the experimental values. Two factors may contribute to this discrepancy: (i) the DFT (B3LYP) method employed to optimize the ground-state structure of **3** usually underestimates the weak metal−metal interaction, thus leading to the longer metal−metal bond length;[68,69] (ii) hydrogen atoms were used in model compound **3** to replace both the *N*-methyl and *C*-aryl groups in compounds **1** and **2**, which, especially those on the nitrogen centers, tend to enhance metal−metal interaction.[70]

The frontier orbitals and nearby MOs from the DFT calculations in ascending order of orbital energy are as follows: $76a_u$ ($\pi(Ru_2) + \pi(C\equiv C)$); $77a_g$ ($\pi^*(Ru_2) + \pi(C\equiv C)$); $77a_u$, $78a_g$,

(65) Yuan, Z.; Stringer, G.; Jobe, I. R.; Kreller, D.; Scott, K.; Koch, L.; Taylor, N. J.; Marder, T. B. *J. Organomet. Chem.* **1993**, *452*, 115.
(66) *Ferrocenes: Homogeneous Catalysis, Organic Synthesis, Materials Science*; Togni, A.; Hayashi, T., Eds.; VCH Publishers: New York, 1995.
(67) Miskowski, V. M.; Hopkins, M. D.; Winkler, J. R.; Gray, H. B. In *Inorganic Electronic Structure and Spectroscopy*; Solomon, E. I., Lever, A. B. P., Eds.; Wiley: New York, 1999; Vol. 2.
(68) Novozhilova, I. V.; Volkov, A. V.; Coppens, P. *J. Am. Chem. Soc.* **2003**, *125*, 1079.
(69) Stoyanov, S. R.; Villegas, J. M.; Rillema, D. P. *J. Phys. Chem. B* **2004**, *108*, 12175.
(70) Pan, O. J.; Zhang, H. X. *Inorg. Chem.* **2004**, *43*, 593.

$79a_g$, and $78a_u$ (π(Fe—C)); $79a_u$ (π(Fe—C)); $80a_g$ ($\pi^*(Ru_2)$, HOMO); $80a_u$ ($\delta^*(Ru_2)$, LUMO); $81a_g$ (σ^*(Ru—C), LUMO+1). The calculated HOMO−LUMO gap is 1.84 eV. Although the low symmetry of **3** (C_i) results in an extensive mixing among valence orbitals that prevents "classical" assignment of MOs to a single atomic center or a molecular fragment, some salient features can be observed. First, the order of the aforementioned MOs reaffirms the previous designation of a $\pi^4\delta^2\pi^{*4}$ configuration for bisalkynyl compounds of a Ru_2(III,III) core, and the large HOMO−LUMO gap is consistent with the diamagnetism observed.[29] Second, four Fc-based MOs lie immediately below the HOMO ($\pi^*(Ru_2)$), verifying the order of sequential one-electron oxidations concluded in the previous communication.[34] Third, the LUMO+1 is predominantly σ^*(Ru—C), which explains the irreversibility of the second reduction observed for all Ru_2(III,III)-bisalkynyl compounds:[61,71] the second reduction populates the Ru—C antibonding orbital and results in the cleavage of a Ru—C bond and disintegration of Ru_2(III,III)-bisalkynyl species.

According to the vertical electron transition mechanism in the absorption process, the optimized ground-state geometry was kept, while the TD-DFT (B3LYP) was performed to calculate excited states relevant to electronic absorptions. With respect to the ^1A_g ground state under the C_i point symmetry, the $^1A_g \rightarrow {}^1A_u$ transitions are dipole-allowed. The tables summarizing calculated low-lying absorptions and corresponding oscillator strengths of **3** for isolated molecules are provided in the Supporting Information. From the TD-DFT calculations, a ^1A_u excited state (mainly contributed by $77a_g \rightarrow 80a_u$) gives rise to an absorption at 840 nm, which, as illustrated by the electron density diagrams in Figure 6a, is best ascribed to the $\pi^*[d_{yz}(Ru_2)] \rightarrow \delta^*[d_{xy}(Ru_2)]$ transition. The blue-shift of the calculated λ_{max} from the experimental value (ca. 910 nm) is attributed to the gas phase calculation, and the correction of solvent effect would significantly red-shift the calculated λ_{max} and yield a better match, as previously demonstrated.[70,72,73] Consistent with the conclusion of the filled−filled π-interaction being dominant in metal-alkynyl compounds,[74] the $\pi^*[d_{yz}(Ru_2)]$ ($77a_g$) orbital contains a substantial contribution of π(C≡C), which renders a partial LMCT character to the transition observed at ca. 910 nm. Although there are many dipole-allowed transitions of energy close to that of intense absorption at ca. 510 nm, the absorption calculated at 409 nm (shown in Figure 6b) from the L(N)→d*(Ru_2), $\delta(Ru_2)$→d*(Ru_2), and $\pi(Ru_2)$ + π(C≡C)→s*(Ru−C) mixed transitions is the best candidate on the basis of its oscillator strength (0.1895).

Spectroelectrochemistry. The spectroelectrochemistry of compound **2a** was reported previously.[34] Spectroelectrochemistry was performed on compounds **2d**, **2c**, and **2b** in 0.20 M Bu_4NPF_6 THF solution, and the spectra of the oxidation products are shown in Figures 7, 8, and 9, respectively. Spectroelectrochemistry to form a given oxidation product yielded absorption spectra with clean isosbestic points, although the reversibility was not ideal. For compounds **2d** and **2c** only partial reversibility (ca. 78% recovery) from the fully oxidized form $\mathbf{2}^{3+}$ to the reduced form **2** was observed. For **2b**, while good reversibility was observed for the first two oxidations, the third oxidation resulted in complete decomposition of the complex ion.

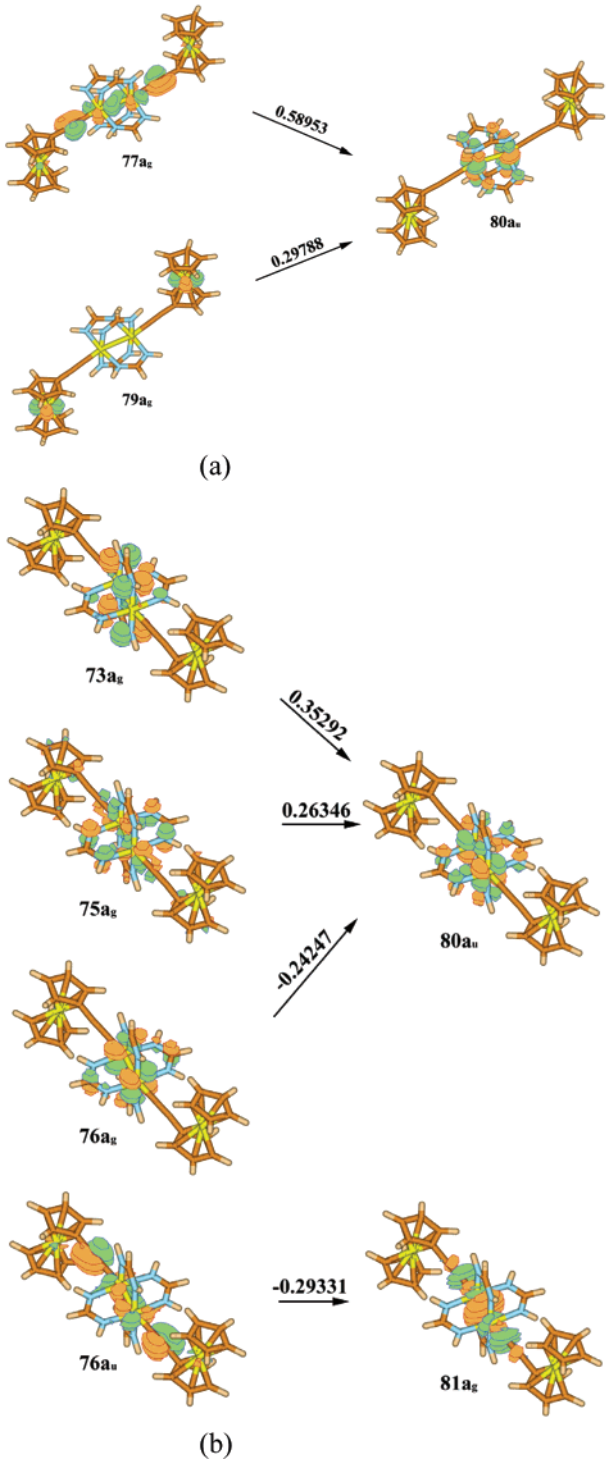

Figure 6. (a) The single electron transitions with |CI coefficient| > 0.1 in the TD-DFT calculations for the 840 nm absorption of compound **3**. (b) The single electron transitions with |CI coefficient| > 0.1 in the TD-DFT calculations for the 409 nm absorption of compound **3** in the gas phase; CI coefficients are placed above the respective arrows.

In Figure 7, the oxidation of **2d** to $\mathbf{2d}^+$ results in a slight energy shift and broadening of bands at 20 200 and 11 390 cm^{-1} and the appearance of new NIR bands centered at approximately 4000 and 5300 cm^{-1}. Further oxidation to $\mathbf{2d}^{2+}$ causes these NIR bands to disappear, and so we assign these NIR bands to intervalence transitions of Fc to Ru_2^{+7}.

(71) Ren, T. *Organometallics* **2002**, *21*, 732.
(72) Pan, Q.-J.; Zhang, H.-X. *Organometallics* **2004**, *23*, 5198.
(73) Pan, Q. J.; Zhang, H. X. *Eur. J. Inorg. Chem.* **2003**, 4202.
(74) Lichtenberger, D. L.; Renshaw, S. K.; Wong, A.; Tagge, C. D. *Organometallics* **1993**, *12*, 3522.

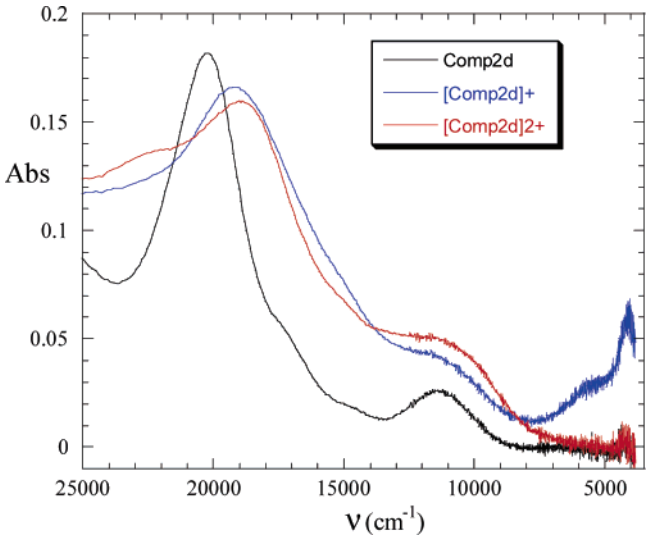

Figure 7. Vis−NIR spectrum of of *trans*-$(FcC_2)Ru_2$(*m*-MeODMBA)$_4$-$(C_2Si^iPr_3)$ (**2d**) and those of spectroelectrochemcally generated **2d**$^+$ and **2d**$^{2+}$ in 0.20 M (*n*-Bu)$_4$NPF$_6$ THF solution.

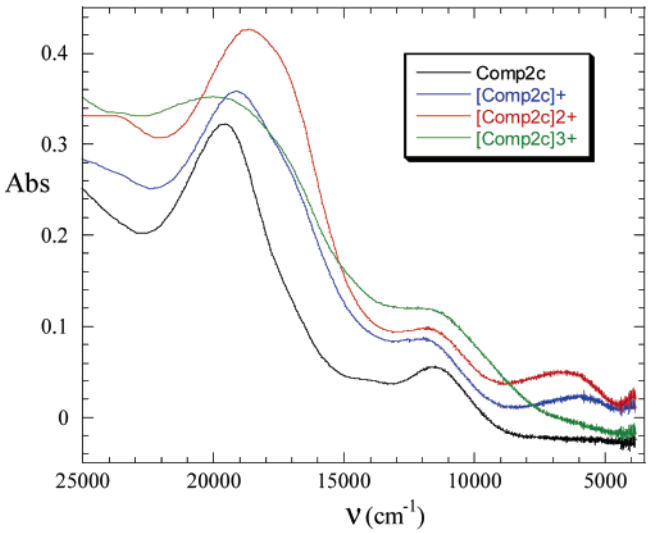

Figure 8. Vis−NIR spectrum of *trans*-Ru_2(*m*-MeODMBA)$_4$$(C_4Fc)_2$ (**2c**) and those of spectroelectrochemcally generated **2c**$^+$, **2c**$^{2+}$, and **2c**$^{3+}$ in 0.20 M (*n*-Bu)$_4$NPF$_6$ THF solution.

Figure 8 shows the spectra of **2c**, **2c**$^+$, **2c**$^{2+}$, and **2c**$^{3+}$. Because of the overlap of the redox couples to form **2c**$^+$ and **2c**$^{2+}$ (**B** + **C** in Figure 4), the spectrum labeled **2c**$^+$ is the result of an equilibrium mixture of **2c**$^+$ and **2c**$^{2+}$. Nevertheless, it is possible to say that the formation of **2c**$^+$ (Fc−Ru^{7+}−Fc) does result in a low energy NIR band at ca. 4000 cm^{-1} and that, with the formation of **2c**$^{2+}$ (Fc−Ru_2^{7+}−Fc$^+$), an additional NIR band grows in at ca. 6250 cm^{-1}. Oxidation to **2c**$^{3+}$ resulted in the loss of these NIR bands, and so these bands are assigned to the two possible intervalence transitions, Fc to Ru_2^{7+} (4000 cm^{-1}) and Fc to Fc$^+$ (6250 cm^{-1}).

Figure 9 shows the spectral transformation of **2b** to **2b**$^+$ and **2b**$^+$ to **2b**$^{2+}$, respectively, while the spectrum of **2b**$^{3+}$ could not be obtained due to its instability. The NIR bands of **2b**$^+$ (Fc_a−Ru_2^{7+}−Fc_b) closely resemble those of **2d**$^+$ in Figure 7 and are assigned to intervalence transitions between Fc and Ru_2^{7+}. The band at 5900 cm^{-1} for **2b**$^{2+}$ (Fc_a−Ru_2^{7+}−Fc_b^+) is assigned to a Fc to Fc$^+$ transition, while the band at 4200 cm^{-1} is a Fc to Ru_2^{7+} IVCT transition.

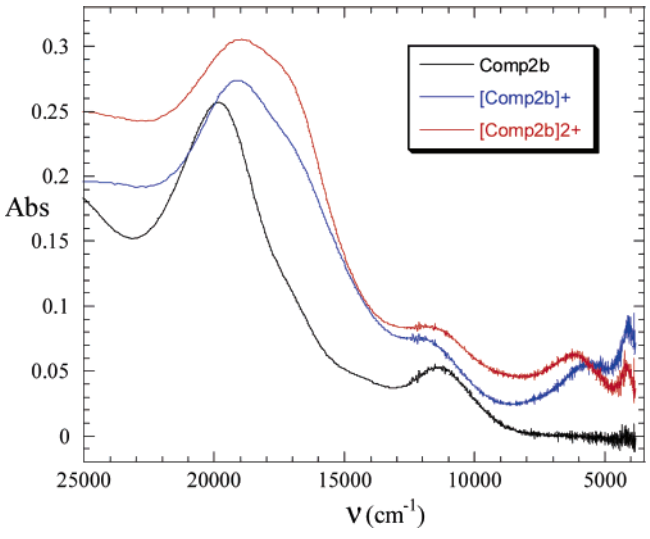

Figure 9. Vis−NIR spectrum of *trans*-Ru_2(*m*-MeODMBA)$_4$$(C_2Fc)(C_4Fc)$ (**2b**) and those of spectroelectrochemcally generated **2b**$^+$, **2b**$^{2+}$, and **2b**$^{3+}$ in 0.20 M (*n*-Bu)$_4$NPF$_6$ THF solution.

Table 3. Spectral Data for Deconvoluted Gaussian Intervalence Bands[a] of Oxidized **2a**−**d**

compd	band I (Fc to Ru_2^{7+}) ν_{max} ($\Delta\nu_{1/2}$, ϵ)	band II (Fc to Fc$^+$) ν_{max} ($\Delta\nu_{1/2}$, ϵ)	reference
2a$^+$	<3800		34
2a^{2+}	<3800	6000 (800, 1000)	34
2b$^{+\,b}$	4040 (310, 2900) 5500 (1530, 3300)		this work
2b^{2+}	4100 (260, 2200)	6230 (1520, 4200)	this work
2c^{+b}	3850 (480, 800) 5560 (1250, 700)	6690 (1780, 1200)	this work
2c^{2+}	3860 (320, 1000)	6680 (1780, 2900)	this work
2d$^+$	4060 (350, 2900) 5250 (1120, 2200)		this work

[a] ν_{max} and $\Delta\nu_{1/2}$ in cm^{-1} and extinction coefficient (ϵ) in M^{-1} cm^{-1}. [b] The spectrum of **2c**$^+$ is a mixture of **2c**$^+$ and **2c**$^{2+}$.

The intervalence transitions of the above complexes were deconvoluted from the electron absorption band envelope by assuming a Gaussian band shape, and the resulting spectral data are compiled in Table 3.

Discussion

The multiple intervalence transitions observed for **2d**$^+$ were not anticipated because there is only one donor−acceptor interaction, and that is between the Fc moiety and Ru_2^{7+}. However, the asymmetry of the Ru_2^{7+} coordination sphere, in which FcC≡C and $^iPr_3$SiC≡C ligands are trans to each other, is expected to remove the distinction between g and u MO symmetries and enables the occurrence of two intervalence excitations. The bandwidths at half-peak height for both bands (Table 3) are far smaller than that predicted by the Hush model ($\Delta\nu_{1/2} = (2310\nu_{max})^{1/2}$),[75] and this suggests that the extent of delocalization is sufficient to classify **2d**$^+$ as a strongly coupled Class II or perhaps Class III system.[76,77]

It was suggested in the preceding communication that compounds **2a**$^+$ and **2a**$^{2+}$ are delocalized with respect to both Fc−Ru_2^{7+}−Fc and Fc$^+$−Ru_2^{7+}−Fc states.[34] This was based not

(75) Hush, N. S. *Prog. Inorg. Chem.* **1967**, *8*, 391.
(76) Robin, M. B.; Day, P. *Adv. Inorg. Chem. Radiochem.* **1967**, *10*, 247.
(77) Demadis, K. D.; Hartshorn, C. M.; Meyer, T. J. *Chem. Rev.* **2001**, *101*, 2655.

Table 4. Voltammetric and Spectroelectrochemical Results Related to {Fc−[M]−Fc$^+$} Mixed Valent Ions

–[M]–	$C_\omega\cdots C_{\omega'}$, Å	ΔE, V	ν(IVCT), cm^{-1}	ϵ, M^{-1} cm^{-1}	$\Delta\nu_{1/2}$, cm^{-1}	$\Delta\nu_{Hush}$,[a] cm^{-1}	ref
none	1.45	0.35	5000	920	3700	3400	78
$-C_2-$	4.0	0.23	6410	670	5000	3850	79
$-C_4-$	6.8	0.10	8470	570	5000	4420	79
$-(CH)_2-$		0.17	4910	1340	4360	3370	80
$-(CH)_4-$		0.13	5500	1570	4340	3560	80
$-(CH)_6-$		0.10	6010	2100	3800	3730	80
$-C_2Ru(dppm)_2C_2-$	9.36	0.22	4770	6700	3300	3320	41
$-C_2Cu_3(dppm)_3C_2-$	8.39	0.11	8000	100	3800	4300	42
$-C_2Pt_2(dppm)_2C_2-$	12.00	0.25	11 300	610	2800	5110	43
$-C_2Ru_2(m\text{MeODMBA})_4C_2-$	11.58	0.30	6000	1000	800	3720	this work
$-C_2Ru_2(m\text{MeODMBA})_4C_4-$	13.84	0.21	6230	4200	1520	3790	this work
$-C_4Ru_2(m\text{MeODMBA})_4C_4-$	16.60	0.27	6680	2900	1780	3930	this work

[a] $\Delta\nu_{Hush} = (2310\nu_{max})^{1/2}$.

only on the magnitude of the free energy of comproportionation ($F\Delta E_c$) but also on the characteristics of the intervalence band that were *inconsistent* with a valence-trapped state. This is illustrated by the data in Table 4, which compares the intervalence data for the complexes of this study to that of ferrocene/ferrocenium type mixed-valence species in the literature. Calculated Hush model IVCT bandwidths are also included in Table 4. For complex **2a**$^{2+}$, the ferrocene to ferrocenium charge-transfer band has a bandwidth $\Delta\nu_{1/2}$ of 800 cm^{-1} which is far less than the value of 3720 cm^{-1} predicted by the Hush model and considerably less than that of the other complexes in Table 4. That this degree of coupling in **2a**$^{2+}$ occurs despite a separation of 11.6 Å between ferrocene and ferrocenium is testimony to the effectiveness of both polyyne and Ru_2^{7+} in superexchange coupling. Indeed, most of the literature Fc−Fc$^+$ pairs, including 1,1′-biferrocene where two Fc units are merely 1.45 Å apart, have IVCT bandwidths that are about the same or larger than the values predicted by the Hush model, further illustrating the proficiency of $Ru_2(DMBA)_4$ unit in mediating electronic coupling.

The bandwidths seen for **2b**$^{2+}$ and **2c**$^{2+}$ in Table 4 are also far narrower than that predicted by the Hush model, and this too is suggestive of a delocalized state. However, for both **2b**$^+$ and **2c**$^+$, two Fc to Ru_2^{7+} transitions (Band I in Table 3) are observed, while, for **2a**$^+$, only a single transition is seen. As mentioned above for **2d**$^+$, asymmetry can lift the distinction between g and u symmetries of valence MOs and allows two Fc to Ru_2^{7+} transitions, and this rationale certainly applies to the unsymmetric compound **2b**$^+$. For the structurally symmetric **2c**$^+$, however, the observed electronic asymmetry arises from a valence-trapped mixed-valence state. If coupling between Fc and Ru_2^{7+} as mediated by a butadiynyl spacer is valence trapped, it is likely that the mixed-valence states of the oxidation products of **2b** and **2c** (Table 3) are also valence trapped albeit very strongly coupled.

In comparing the mixed-valence ions of the symmetric compounds **2a** with **2c**, it seems clear that the butadiynyl spacers attenuated coupling compared to ethynyl but to what extent? In our earlier study of compounds in which two Ru_2 termini were bridged by polyyn-diyls, a decay factor of $\gamma = 0.064$ Å^{-1} in resonance exchange was estimated according to the equation

$$H_{ad} = H_o \exp(-\gamma R) \tag{4}$$

where H_o is the resonance exchange at donor−acceptor wave function overlap and R is the separation between donor and acceptor.[32] Using a value of $\gamma = 0.064$ Å^{-1}, eq 4 predicts a drop in resonance exchange of only 27% when going from ethynyl to butadiynyl spacers in complexes **2a** and **2c**, respectively. For the Class III system, **2a**$^{2+}$, extracting the resonance exchange value for the Fc to Fc$^+$ IVCT transition is simply one-half the energy at band maximum or $H_{ad} = 3000$ cm^{-1}. For a strongly coupled valence-trapped system, the Hush model gives values of resonance exchange that are too small because delocalization decreases the dipole moment length. It is possible to extract resonance exchange values from comproportionation data, but several approximations have to be made.[81]

The free energy of comproportionation associated with the Fc to Fc$^+$ IVCT transition of **2c**$^{2+}$ is simply the difference in Fc oxidation couples or 0.27 V (2180 cm^{-1}). The factored expression for the free energy of comproportionation ΔG_c is given by[81]

$$\Delta G_c = \Delta G_s + \Delta G_e + \Delta G_i + \Delta G_r + \Delta G_{ex} \tag{5}$$

where ΔG_s reflects the statistical distribution of the comproportionation equilibrium, ΔG_e accounts for the electrostatic repulsion between like-charged metal centers, ΔG_i is an inductive factor dealing with competitive coordination of the bridging ligand by the metal ions, ΔG_r is the free energy of resonance exchange; and ΔG_{ex} is the antiferromagnetic exchange term that results when exchange stabilizes the unpaired electrons of **2**$^{2+}$. The expression relating resonance exchange to the free energy of resonance exchange is approximated by[81]

$$\Delta G_r' = \frac{H_{ad}^{\ 2}}{E_{IT}} \tag{6}$$

where $2\Delta G_r' = \Delta G_r$..

Antiferromagnetic exchange through short carbon-rich bridges is on the order of 30−40 cm^{-1},[33] and sufficiently small to be ignored. The nonresonance contributions to the free energy of comproportionation ($\Delta G_{nr} = \Delta G_s + \Delta G_e + \Delta G_i$) are on the order of 500 cm^{-1}, as have been found for other mixed-valence systems.[81] Under these approximations, a $\Delta G_r'$ value of 840 cm^{-1} is obtained from $\Delta G_r' = {}^1/_2(\Delta G_c - 500\ \text{cm}^{-1}) = {}^1/_2(2180-500)$. Placing this value in eq 6 and $E_{IT} = 6680$ yields

(78) Powers, M. J.; Meyer, T. J. *J. Am. Chem. Soc.* **1978**, *100*, 4393.
(79) Levanda, C.; Bechgaard, K.; Cowan, D. O. *J. Org. Chem.* **1976**, *41*, 2700.
(80) Ribou, A. C.; Launay, J. P.; Sachtleben, M. L.; Li, H.; Spangler, C. W. *Inorg. Chem.* **1996**, *35*, 3735.
(81) Evans, C. E. B.; Naklicki, M. L.; Rezvani, A. R.; White, C. A.; Kondratiev, V. V.; Crutchley, R. J. *J. Am. Chem. Soc.* **1998**, *120*, 13096.

$H_{ad} = 2400\ cm^{-1}$. This value is a 20% drop in H_{ad} compared to that found for $\mathbf{2a}^{2+}$ in acceptable agreement with the 27% decrease predicted for polyyne spacers as discussed above. While this is only a single calculation, the results indicate that attenuation of coupling in polyyne/Ru_2 chain systems is essentially additive and this has consequences for the purposeful construction of electronic devices based on these materials.

Conclusions

We have demonstrated the exceptional ability of the $Ru_2(DMBA)_4$ unit in mediating electron mobility between ferrocenium and ferrocene reporter groups by voltammetric and spectroelectrochemical studies of the *trans*-$(FcC_{2n})Ru_2(Y\text{-}DMBA)_4(C_{2m}Fc)$ series. These results and that obtained from earlier study of charge transfer across carbon-rich bridges[32,33] provide the validation of our proposal to realize molecular wires based on Ru_2-alkynyl oligomers (Scheme 1). In addition to the continued efforts in the synthesis and characterization of these oligomers, we are also interested in the possibility of attenuating the charge-transfer event through both the covalent and noncovalent modifications of the Ru_2-alkynyl moiety and controlling the direction of charge transfer (rectification) through donor/acceptor functionalization.

Experimental Section

$Ru_2(DMBA)_4Cl_2$, $Ru_2(m\text{-}MeODMBA)_4Cl_2$, and ethynylferrocene were prepared as previously described.[61,64,82] Triisopropylsilylacetylene and *n*BuLi were purchased from Aldrich, and silica gel was from Merck. 1-Ferrocenyl-4-trimethylsilyl-1,3-butadiyne was prepared from the coupling reaction between ethynylferrocene and trimethylsilylacetylene under Hay conditions (see the Supporting Information). THF was distilled over Na/benzophenone under an N_2 atmosphere prior to use. ^{1}H and ^{13}CNMR spectra were recorded on a Bruker AVANCE300 NMR spectrometer with chemical shifts (δ) referenced to the residual $CHCl_3$ and the solvent $CDCl_3$, respectively. Mass spectra (FAB, nitrobenzyl alcohol matrix) were recorded on a VG Trio-2 mass spectrometer. Infrared spectra were recorded on a Perkin-Elmer 2000 FT-IR spectrometer using KBr disks. Vis-NIR spectra were acquired in THF using a Perkin-Elmer Lambda-900 UV−vis−NIR spectrophotometer. Both cyclic and differential pulse voltammograms were recorded in 0.2 M $(n\text{-}Bu)_4NPF_6$ solution (THF, N_2-degassed) on a CHI620A voltammetric analyzer with a glassy carbon working electrode (diameter = 2 mm), a Pt-wire auxiliary electrode, and a Ag/AgCl reference electrode. The concentration of diruthenium species is always 1.0 mM. The ferrocenium/ferrocene couple was observed at 0.568 V (vsAg/AgCl) under experimental conditions.

Preparation of $Ru_2(DMBA)_4(C_2Fc)_2$ (1a). To a 40 mL THF solution of $Ru_2(DMBA)_4Cl_2$ (0.173 g, 0.20 mmol) was added 5 equiv of LiC_2Fc (prepared from treating 1 mmol of FcC_2H with *n*BuLi) at room temperature. The reaction mixture was stirred under argon for 3 h and then filtered through a 2 cm silica gel pad to yield a dark red solution. After the solvent removal, the residue was washed with copious amounts of methanol and hexanes and dried under vacuum overnight to yield 0.205 g of red powder (85% based on Ru). Data for **1a**: Anal. for $C_{60}H_{62}Fe_2N_8Ru_2{\cdot}C_4H_8O$, Found (Calcd): C, 60.10 (60.00); H, 5.29 (5.47); N, 8.45 (8.75); ^{1}HNMR: 7.43−7.36 (*m*, 12H, benzene), 7.02−6.98 (*m*, 8H, benzene), 4.10 (*t*, 4H, Fc), 4.03 (*s*, 10H, Fc), 3.95 (*t*, 4H, Fc), 3.30 (*s*, 24H, C**H**$_3$N); ^{13}CNMR (C≡C): 118.7, 70.4; MS−FAB (*m*/*e*, based on ^{101}Ru): 1211[M^+H]; vis−NIR, λ_{max}(nm, $\epsilon(M^{-1}\ cm^{-1})$): 894 (1194), 495 (9068); IR, υ(C≡C)/cm^{-1}: 2081(s).

Preparation of $Ru_2(DMBA)_4(C_2Fc)(C_4Fc)$ (1b) and $Ru_2(DMBA)_4(C_4Fc)_2$ (1c). To a 40 mL THF solution of $Ru_2(DMBA)_4Cl_2$ (0.120 g, 0.15 mmol) was added a mixture of LiC_2Fc and LiC_4Fc (prepared from the reaction of a mixture of 0.15 mmol of FcC_2H and 0.30 mmol of FcC_4TMS with *n*BuLi) at room temperature. The reaction mixture was stirred under argon for 3 h. After solvent removal, the residue was loaded on a silica gel column and eluted with THF−hexanes (2:10, v/v) to yield a trace amount of $Ru_2(DMBA)_4(C_2Fc)_2$ (**1a)**, 0.040 g of $Ru_2(DMBA)_4(C_2Fc)(C_4Fc)$ (**1b**, 22% based on Ru), and 0.045 g of $Ru_2(DMBA)_4(C_4Fc)_2$ (**1c**, 24% based on Ru). Data for **1b**: Anal. for $C_{62}H_{62}Fe_2N_8Ru_2{\cdot}2C_4H_8O_2{\cdot}3H_2O$, Found (Calcd): C, 57.18 (57.46); H, 5.60 (5.79); N, 7.57 (7.60). ^{1}HNMR: 7.43−7.37 (*m*, 12H, benzene), 7.00−6.97 (*m*, 8H, benzene), 4.29 (*t*, 2H, Fc), 4.13 (*s*, 5H, Fc), 4.10 (*t*, 2H, Fc), 4.06 (*t*, 2H, Fc), 4.03 (*s*, 5H, Fc), 3.96 (*t*, 2H, Fc), 3.26 (*d*, 24H, C**H**$_3$N); ^{13}CNMR (C≡C): 132.6, 125.6, 125.0, 67.4, 66.4, 65.6; MS−FAB (*m*/*e*, based on ^{101}Ru): 1234[M^+]; vis−NIR, λ_{max}(nm, $\epsilon(M^{-1}\ cm^{-1})$): 902 (1690), 505 (12010); IR, υ(C≡C)/cm^{-1}: 2173(s), 2029-(s). Data for **1c**: Anal. for $C_{64}H_{62}Fe_2N_8Ru_2{\cdot}2C_4H_8O{\cdot}H_2O$, Found (Calcd): C, 59.35(59.59); H, 5.58(5.52); N, 7.36(7.72). ^{1}HNMR: 7.42−7.39 (*m*, 12H, benzene), 6.98−6.95 (*m*, 8H, benzene), 4.29 (*t*, 4H, Fc), 4.13 (*s*, 10H, Fc), 4.07 (*t*, 4H, Fc), 3.24 (*s*, 24H, C**H**$_3$N); MS−FAB (*m*/*e*, based on ^{101}Ru): 1258[M^+]; vis−NIR, λ_{max}(nm, $\epsilon(M^{-1}\ cm^{-1})$): 911 (1290), 514 (9520); IR, υ(C≡C)/cm^{-1}: 2171(s), 2026(s).

Preparation of $Ru_2(m\text{-}MeODMBA)_4(C_2Fc)_2$ (2a). Compound **2a** was prepared using the same procedure as that for **1a** with $Ru_2(DMBA)_4Cl_2$ being replaced by $Ru_2(m\text{-}MeODMBA)_4Cl_2$ in 91% yield. Data for **2a**: Anal. for $C_{64}H_{70}Fe_2N_8O_4Ru_2{\cdot}C_6H_{14}$ Found (Calcd): C, 59.48(59.40); H, 5.99(5.98); N, 8.28(7.92). ^{1}HNMR: 7.43−7.37 (*m*, 4H, benzene), 6.97−6.94 (*m*, 4H, benzene), 6.65−6.57 (*m*, 8H, benzene), 4.15 (*s*, 4H, Fc), 4.09 (*s*, 10H, Fc), 4.01 (*s*, 4H, Fc), 3.81 (*s*, 12H, C**H**$_3$O), 3.35 (*s*, 24H, C**H**$_3$N); ^{13}CNMR (C≡C): 122.5, 72.2; MS−FAB (*m*/*e*, based on ^{101}Ru): 1124[M^+H−C_2Fc]; vis−NIR, λ_{max}(nm, $\epsilon(M^{-1}\ cm^{-1})$): 899 (1415), 495 (10 270); IR, υ(C≡C)/cm^{-1}: 2083(m).

Preparation of $Ru_2(m\text{-}MeODMBA)_4(C_2Fc)(C_4Fc)$ (2b) and $Ru_2(m\text{-}MeODMBA)_4(C_4Fc)_2$ (2c). To a 40 mL THF solution of $Ru_2(m\text{-}MeODMBA)_4Cl_2$ (0.310 g, 0.32 mmol) was added a mixture of LiC_2Fc and LiC_4Fc (prepared from the reaction of a mixture of 0.32 mmol of FcC_2H and 0.64 mmol of FcC_4TMS with *n*BuLi) at room temperature. The reaction mixture was stirred under argon for 3 h. After solvent removal, the residue was loaded on a silica gel column and eluted with THF/hexanes (3:10−5:10, v/v) to yield a trace amount of **2a**, 0.106 g of **2b** (25% based on Ru), and 0.050 g of **2c** (12% based on Ru).

Data for $Ru_2(m\text{-}MeODMBA)_4(C_2Fc)(C_4Fc)$ (2b): Anal. for $C_{66}H_{70}Fe_2N_8O_4Ru_2{\cdot}C_4H_8O$ Found (Calcd): C, 59.33 (58.99); H, 5.61 (5.48); N, 8.07 (7.87). ^{1}HNMR: 7.38 (*t*, 4H, benzene), 6.96−6.93 (*m*, 4H, benzene), 6.62−6.54 (m, 8H, benzene), 4.34 (*t*, 2H, Fc), 4.18 (*s*, 5H, Fc), 4.15 (*t*, 2H, Fc), 4.11 (*t*, 2H, Fc), 4.07 (*s*, 5H, Fc), 4.01 (*t*, 2H, Fc), 3.83 (*d*, 12H, C**H**$_3$O), 3.31 (*s*, 24H, C**H**$_3$N); ^{13}CNMR (C≡C): 130.3, 121.1, 71.1, 70.1, 69.4, 67.4; MS−FAB (*m*/*e*, based on ^{101}Ru): 1354[M^+]; vis−NIR, λ_{max}(nm, $\epsilon(M^{-1}\ cm^{-1})$): 901 (2210), 504 (15640); IR, υ(C≡C)/cm^{-1}: 2170(s), 2085(m), 2024(s).

Data for $Ru_2(m\text{-}MeODMBA)_4(C_4Fc)_2$ (2c): Anal. for $C_{68}H_{70}Fe_2N_8O_4Ru_2{\cdot}C_6H_{14}$, Found (Calcd): C, 60.72 (60.74); H, 5.53 (5.79); N, 7.46 (7.66). ^{1}HNMR: 7.38 (*t*, 4H, benzene), 6.97−6.94 (*m*, 4H, benzene), 6.60−6.52 (*m*, 8H, benzene), 4.34 (*t*, 4H, Fc), 4.18 (*s*, 10H, Fc), 4.12 (*t*, 4H, Fc), 3.83 (s, 12H, C**H**$_3$O), 3.28 (*s*, 24H, C**H**$_3$N); ^{13}CNMR (C≡C): 137.2, 130.4, 72.4, 69.9; MS−FAB (*m*/*e*, based on ^{101}Ru): 1378[M^+]; vis−NIR, λ_{max}(nm, $\epsilon(M^{-1}\ cm^{-1})$): 915 (1880), 513 (13260); IR, υ(C≡C)/cm^{-1}: 2173 (s), 2028 (s).

Preparation of $Ru_2(m\text{-}MeODMBA)_4(C_2Si^iPr_3)(C_2Fc)$ (2d). To a 40 mL THF solution of $Ru_2(m\text{-}MeODMBA)_4Cl_2$ (0.310 g, 0.32 mmol) was added a mixture of $LiC_2Si^iPr_3$ and LiC_2Fc (prepared from the reaction of a mixture of 0.32 mmol of $^iPr_3SiC_2H$ and 0.64 mmol of FcC_2H with *n*BuLi) at room temperature. The reaction mixture was stirred under argon for 3 h. After solvent removal, the residue was

(82) Doisneau, G.; Balavoine, G.; Fillebeen-Khan, T. *J. Organomet. Chem.* **1992**, *425*, 113.

loaded on a silica gel column and eluted with THF/hexanes (2:10−4:10, v/v) to yield 0.085 g of Ru_2(*m*-MeODMBA)$_4$($C_2Si^iPr_3$)$_2$ (21% based on Ru), 0.180 g of **2d** (43% based on Ru), and a trace amount of **2a**. Data for **2d**: Anal. For $C_{63}H_{82}FeN_8O_4Ru_2Si$ Found (Calcd): C, 58.43 (58.15); H, 6.66 (6.31); N, 8.59 (8.62). ^{1}HNMR: 7.39 (*t*, 4H, benzene), 7.00−6.90 (*m*, 4H, benzene), 6.64−6.54 (*m*, 8H, benzene), 4.14−4.00 (*m*, 9H, Fc), 3.83 (*s*, 12H, C**H**$_3$O), 3.33 (*d*, 24H, C**H**$_3$N), 1.08−0.93 (*m*, 21H, (C$_3$**H**$_7$)$_3$Si); ^{13}CNMR (C≡C): 138.2, 131.7, 114.7, 70.9; MS−FAB (*m*/*e*, based on ^{101}Ru): 1303[M^+H]; vis−NIR, λ_{max}(nm, ϵ(M^{-1} cm^{-1})): 878 (2170), 495 (14690); IR, υ(C≡C)/cm^{-1}: 2084-(m), 2002(s).

Computation Details of 3. The structure of **3** in the ground state was fully optimized using the density functional method, B3LYP (Becke's 3 parameter hybrid functional using the Lee−Yang−Parr correlation functional).[83−86] Based on the optimized structure, TD-DFT (time-dependent density functional theory) method[87,88] was performed to calculate excited states related to absorption spectra of compounds **1** and **2**. In these calculations, **3** retains a C_i symmetry consistent with X-ray structures of **1a**−**1c**. In the calculations, quasi-relativistic pseudopotentials of the Ru and Fe atoms proposed by Hay and Wadt[89,90] with 16 and 16 valence electrons, respectively, are employed and the LanL2DZ basis sets associated with the pseudopotential are adopted. All the calculations are performed using the *Gaussian03* program package on an Origin 3800 server.[91]

Spectroelectrochemistry of 2a−**2d**. An OTTLE cell was used to perform the spectroelectrochemistry at ambient temperatures.[92] The cell had interior dimensions of roughly 1 × 2 cm^2 with a path length of 0.2 mm and was fitted with a Ag/AgCl reference electrode and ITO (indium−tin oxide) coated glass for the working and counter electrodes. All of the spectroelectrochemical transformations showed good reversibility (greater than 95% recovery of original complex spectrum).

X-ray Data Collection, Processing, and Structure Analysis and Refinement. Single crystals **1a**, **1b**, and **1c** were grown via slow diffusion of hexanes into a THF solution (**1a**), a benzene solution (**1b**), or a toluene solution (**1c**). X-ray intensity data were measured at 300 K on a Bruker SMART1000 CCD-based X-ray diffractometer system using Mo Kα (λ = 0.710 73 Å). Data were measured using omega scans of 0.3° per frame such that a hemisphere (1271 frames) was collected. No decay was indicated for any of the three data sets by the recollection of the first 50 frames at the end of data collections. The frames were integrated with the Bruker SAINT software package[93] using a narrow-frame integration algorithm, which also corrects for the Lorentz and polarization effects. Absorption corrections were applied using SADABS supplied by George Sheldrick.

The structures were solved and refined using the Bruker SHELXTL (version 5.1) software package[94] in space groups $P2_1/c$ (**1a**) and $P\bar{1}$ (**1b** and **1c**). Positions of all non-hydrogen atoms of diruthenium moieties were uncovered using a direct method. The asymmetric unit of each of three crystals contains one independent molecule. In the crystal of **1c**, one of the Fc units and the toluene solvent molecule were found to be disordered. The disordered moieties were refined accordingly with distance constraints, and an occupancy ratio of 0.54/0.46 was obtained for the disordered Fc unit. The methyl group on the toluene molecule was constrained to an ideal geometry and allowed to rotate freely about the C−C bond. A similarity restraint (SAME) was used for the chemically equivalent disordered congeners. With all non-hydrogen atoms being anisotropic and all hydrogen atoms in a calculated position and riding mode, the structure was refined to convergence by a least-squares method on F^2, SHELXL-93, incorporated in SHELXTL.PC V 5.03. Relevant information on the data collection and the figures of merit of final refinement are listed in Table 5.

Table 5. Crystal Data for Compounds **1a**, **1b**, and **1c**

	1a	**1b**·0.5C_6H_6	**1c**·C_7H_8
empirical formula	$C_{60}H_{62}Fe_2N_8Ru_2$	$C_{65}H_{68}Fe_2N_8Ru_2$	$C_{71}H_{70}Fe_2N_8Ru_2$
formula weight	1209.02	1275.11	1349.19
space group	$P2_1/c$	$P\bar{1}$	$P\bar{1}$
a (Å)	20.363(2)	10.9105(5)	12.200(1)
b (Å)	19.415(2)	16.6264(8)	14.968(1)
c (Å)	13.870(1)	18.1033(9)	18.298(1)
α (deg)		94.6770(10)	83.358(1)
β (deg)	94.400(2)	105.6250(10)	74.311(1)
γ (deg)		109.0740(10)	84.788(1)
V (Å^3)	5466.9(9)	2936.7(2)	3189.1(3)
Z	4	2	2
ρ_{calc} (g cm^{-3})	1.469	1.442	1.405
μ (mm^{-1})	1.108	1.036	0.958
R1, wR2	0.067, 0.174	0.053, 0.117	0.053, 0.074

Acknowledgment. Work described here is supported by the National Science Foundation (CHE0242623 to T.R.), the Natural Sciences Engineering Research Council of Canada (NSERC to R.J.C.), and the Natural Science Foundation of China (20173021 to H.X.Z.). G.-L.X and M.C.D. thank the University of Miami for a Maytag graduate fellowship and NSERC for a postgraduate scholarship, respectively.

Supporting Information Available: Text containing complete refs 5 and 91, CV and DPV plots and vis-NIR spectra for compounds **1a**−**1c**, synthesis of FcC_4SiMe_3, and details of density functional calculations, and X-ray crystallographic files in CIF format for the structure determination of compounds **1a**, **1b**, and **1c**. This material is available free of charge via the Internet at http://pubs.acs.org.

JA0534452

(83) Pople, J. A.; Gill, P. M. W.; Johnson, B. G. *Chem. Phys. Lett.* **1992**, *199*, 557.
(84) Johnson, B. G.; Frisch, M. J. *J. Chem. Phys.* **1994**, *100*, 7429.
(85) Johnson, B. G.; Frisch, M. J. *Chem. Phys. Lett.* **1993**, *216*, 133.
(86) Stratmann, R. E.; Burant, J. C.; Scuseria, G. E.; Frisch, M. J. *J. Chem. Phys.* **1997**, *106*, 10175.
(87) Bauernschmitt, R.; Ahlrichs, R. *Chem. Phys. Lett.* **1996**, *256*, 454.
(88) Matsuzawa, N. N.; Ishitan, A.; Dixon, D. A.; Uda, T. *J. Phys. Chem. A* **2001**, *105*, 4953.
(89) Wadt, W. R.; Hay, P. J. *J. Chem. Phys.* **1985**, *82*, 284.
(90) Hay, P. J.; Wadt, W. R. *J. Chem. Phys.* **1985**, *82*, 299.
(91) Frisch, M. J. et al. *Gaussian 03*, revision B.03; Gaussian, Inc.: 2003.
(92) Krejcik, M.; DanImagek, M.; Hartl, F. *J. Electroanal. Chem.* **1991**, *317*, 179.
(93) *SAINT V 6.035 Software for the CCD Detector System*; Bruker-AXS Inc., 1999.
(94) *SHELXTL 5.03 (WINDOW-NT Version), Program library for Structure Solution and Molecular Graphics*; Bruker-AXS Inc: 1998. (b) Sheldrick, G. M. *SHELXL-93, Program for the Refinement of Crystal Structures*; University of Göttigen: Germany, 1993. (c) Sheldrick, G. M. *SHELXS-90, Program for the Solution of Crystal Structures*; University of Göttigen: Germany, 1990.